Polymers for Advanced Technologies

WILEY

polymers for advanced technologies

RESEARCH ARTICLE OPEN ACCESS

Soybean Oil-Based Bioadhesive: An Alternative to Sutures

Thaís Franco Simas[1] | Tatiane Araujo Soares[1] | Bruna Carolina Dorm[1] | André Capaldo Amaral[1] | Wilton Rogério Lustri[1] | Luís Geraldo Vaz[2] | Leandro Fernandes[2] | Eliane Trovatti[1]

[1]University of Araraquara-UNIARA, Araraquara, Brazil | [2]Department of Dental Materials and Prosthodontics, Faculty of Dentistry of Araraquara, São Paulo State University (UNESP), Araraquara, Brazil

Correspondence: Eliane Trovatti (elianetrov@yahoo.com.br)

Received: 27 June 2025 | **Revised:** 10 October 2025 | **Accepted:** 13 October 2025

Funding: The authors thank Fapesp for the grant 2017-18782-6 and 2019/25316-7, CNPq grant number 305518/2023-2, and CAPES for Tatiane Araujo Soares PhD grant 88870713632/2022-00.

Keywords: bioadhesives | photopolymerization | soybean oil

ABSTRACT

Sutures are the main tissue approximation technique used in surgical procedures. However, they are operator-dependent and susceptible to inflammatory reactions. In this context, surgical bioadhesives have been developed with the aim of replacing sutures or acting as a complementary protection to them. To fulfill these purposes, bioadhesives need to have specific structural characteristics, such as good tissue adhesion, the ability to aid the healing process without releasing toxic substances or altering the wound microenvironment. Soybean oil stands out as a promising material for the development of bioadhesives due to its favorable structural properties and low cost, which makes its use economically viable. The aim of this study was to develop a bioadhesive based on commercial soybean oil so that it can be used to reinforce sutures or as a tissue bonding agent. The bioadhesive was characterized by FTIR, ^{1}H NMR, rheological analysis, curing time, water absorption, hydrolytic degradation and cytotoxicity. The bioadhesive exhibited 69–80 s curing time, easy handling and malleability, transparency, and low toxicity, with cell viability of approximately 91% after 24 h of exposure to the PolyOSEA film extract. These results show its bioadhesive potential to be used in the healing process of surgical wounds or further biomedical applications.

1 | Introduction

Sutures are currently regarded as the gold standard for the closure of surgical incisions, as the term "suture" encompasses any material utilized to approximate tissues, thereby promoting healing by first intention [1]. A broad range of suture threads is available, including monofilament and multifilament variants. These are further classified according to their origin in natural or synthetic and their tensile strength retention in absorbable, which gradually lose tensile integrity, and non-absorbable, which retain it over time. The ideal suture material should be both malleable and flexible, permitting secure knot formation while eliciting minimal inflammatory response upon contact with biological tissues, ultimately yielding predictable clinical outcomes. However, despite their routine use in medical practice, sutures present numerous drawbacks, including the potential for infection, exposure of the patient to anesthesia, and complications such as wound dehiscence, adhesions, fistulas, and granulomas [2]. These issues are often compounded by variability in surgical technique among practitioners, resulting in inconsistent clinical outcomes. In light of these limitations, there is a growing need for the development of alternative technologies for surgical wound closure [3].

Surgical adhesives are needle-free materials developed with the intent to supplement or replace sutures, thereby mitigating their associated disadvantages. These materials can adhere by molecular bonds between their structures and that of the target tissue [4]. Typically available in liquid or gel form, their solidification ensures stable adhesion of juxtaposed tissue surfaces

[5]. Tissue adhesives can be composed of either synthetic or natural compounds, including cyanoacrylates, poly(ethylene glycol), dendrimers, polysaccharides, and proteins. Nevertheless, several of these formulations present limitations. For instance, while cyanoacrylates are widely employed, they may exhibit tissue toxicity due to their degradation by-products and often result in brittle or overly rigid cured products [6, 7]. Among the natural-based surgical adhesives, fibrin glue (Tisseel—Baxter, Deerfield, IL, USA) provides hemostasis, sealing, and adhesion simultaneously [8]. Despite its use in several surgical procedures, its most significant contribution is in abdominal surgery as a suture reinforcement [9]. BioGlue is a tissue adhesive composed of purified bovine albumin and glutaraldehyde, produced by Cryolife [10]. Initially employed for strengthening vascular anastomoses, it is currently used in cardiac surgery, neurosurgery, and urological surgery as suture protectors [11]. In addition to these commercially available bioadhesives, novel formulations have been studied, including those based on chitosan and on L-3,4-dihydroxyphenylalanine (L-DOPA), a compound found in mussels. However, it should be noted that these formulations are still in the clinical trial stage for use in humans [12]. With respect to plant oil-based bioadhesives, the simple reaction between epoxidized soybean oil (ESO), methacrylic acid, and tannic acid, followed by the addition of zinc ions, was recently published. This bioadhesive can be rapidly cured in situ at the lesion site via photocrosslinking under ultraviolet light-emitting diode (UV-LED) irradiation, demonstrating high adhesion performance under wet conditions [13].

Formulations combining highly biocompatible natural polymers, such as gelatin and alginate, have been studied for use as double composite bioadhesives, resulting in a material with good mechanical properties, high tissue adhesion, and biological compatibility [14]. A bioadhesive formulation based on a combination of gelatin and alginate cross-linked with carbodiimide (*N*-(3-dimethylaminopropyl)-*N*-ethylcarbodiimide hydrochloride [EDC]) and loaded with the hemostatic agent kaolin was investigated for epidermal closure of long surgical incisions ($\geq$4 cm) in a porcine skin model [15].

Oils are water-insoluble substances that remain in a liquid state at ambient temperatures and may originate from vegetable, animal, synthetic, or mineral sources [16]. Vegetable oils, typically extracted from plant seeds, are renewable feedstocks primarily composed of triglycerides, which consist of a glycerol backbone (propane-1,2,3-triol) esterified with three long-chain fatty acids. The defining feature of fatty acids that makes them suitable precursors for polymer production is the presence of unsaturated bonds. These sites of unsaturation allow for diverse structural modifications, each producing distinct physicochemical properties [17]. Soybean (*Glycine max*) is a major global commodity, valued for both its protein content and oil. Despite initially being a by-product of soybean meal production, soybean oil is one of the most used vegetable oils worldwide [18]. From a biochemical standpoint, soybean oil is rich in unsaturated fatty acids—primarily linoleic and linolenic acids—making it particularly attractive for biotechnological applications. The presence of unsaturation ensures that the oil remains in a liquid state even when subjected to significant temperature variations [19, 20]. However, the native reactivity of soybean oil is insufficient for direct photopolymerization, due to the low reactivity of its double bonds. To enhance its suitability as a polymer precursor, it must undergo chemical modifications that introduce reactive functional groups, such as esters or additional unsaturation. One such modification is epoxidation, in which hydrogen peroxide reacts with the carbon–carbon double bonds to form cyclic ethers (epoxides) by incorporating oxygen atoms. Another approach is acrylation, which involves the addition of acrylate groups, thereby rendering the molecule sufficiently reactive for photopolymer-induced solidification [17]. Photopolymerization refers to the polymerization of a reactive resin upon exposure to electromagnetic radiation. This process requires the presence of photoinitiators—compounds that absorb visible light and generate reactive species that initiate polymer formation [21, 22].

The objective of the present study is to synthesize a light-curable polymer derived from the epoxidation and acrylation of soybean oil—a low-cost, renewable resource—with the aim of evaluating its potential as a bioadhesive. This material may serve as a complementary or even alternative solution to conventional suturing techniques. The main innovative contribution of this work, compared with photocurable adhesives and other existing systems, is the use of soybean oil as the polymer matrix, with the advantage of its natural source, wide availability, and low cost, combined with the easy synthesis route, resulting in reduced expenses and improved properties. Although research into oil-based polymers has progressed significantly, further exploration is warranted, given the exceptional versatility of vegetable oils and their potential to offer sustainable, functional alternatives to traditional medical materials.

2 | Materials and Methods

2.1 | Materials

Commercial soybean oil was purchased from Liza (Primavera do Leste, Mato Grosso, Brazil). *N,N*-dimethylacrylamide and diphenylphosphoryl (mesityl)methanone were purchased from AmBeed (Arlington Heights, Illinois, USA). Sodium Carbonate Anhydrous PA ACS (Na_2CO_3), Acrylic Acid ($C_3H_4O_2$), Glacial Acetic Acid PA ACS (CH_3COOH), Hydrogen Peroxide 35% 130V, and Triethylamine P.S ($C_6H_{15}N$). P.A (H_2O_2) were purchased from Êxodo Científica (Sumaré, São Paulo, Brazil). Hydroquinone P.A. ($C_6H_6O_2$) was purchased from LabSynth (Diadema, São Paulo, Brazil). Dimethyl Sulfoxide-d6 was purchased from Sigma-Aldrich, San Luis, Missouri, USA.

2.2 | Methods

2.2.1 | Epoxidation of Soybean Oil

The preparation of ESO followed the procedure described in the literature [17]. Commercial soybean oil (209 g), toluene (50 mL), and glacial acetic acid (15.7 g) were placed into a 500 mL round-bottom flask and maintained in an oil bath at 85°C. Hydrogen peroxide (35% w/w, 90 g) was then gradually added to the flask using a dropping funnel, and the reaction mixture was maintained for 48 h. The mixture was washed with 100 mL of an aqueous sodium carbonate solution (Na_2CO_3, 10% wt), filtered, and dried in an oven at 70°C–80°C.

2.2.2 | Acrylation of the Epoxidised Soybean Oil

ESO (63 g), toluene (20 mL), acrylic acid (16.8 g), and hydroquinone (0.01 g) were mixed, placed in a 500 mL round-bottomed flask, and heated to 85°C for 30 min. Triethylamine (2.8 g) was added to the flask, and the reaction was maintained for a further 2 h at 85°C. The resulting product was washed with ethanol (100 mL, PA), an aqueous sodium carbonate solution (100 mL), and finally with a sodium chloride solution (10% wt, 100 mL). Each washing step was carried out in a separating funnel. Following the washing procedures, the acrylated oil was dried in an oven at 60°C to ensure complete removal of residual water. The product was named AESO.

2.2.3 | Photopolymerisation of AESO

AESO was mixed with *N,N*-dimethylacrylamide and the photoinitiator diphenylphosphoryl (mesityl)methanone. After homogenization, 200 μL of the mixture was put onto a flat surface, and the 2 × 2 cm samples were irradiated with UV light (Delpho instruments, 400 nm, São Carlos, SP) at a distance of 2 cm for polymerization. Six compositions were tested to optimize the concentrations of each component, aiming to produce a film with the desired texture and properties for application as a bioadhesive. The component ratios of AESO: *N,N*-dimethylacrylamide: photoinitiator (in g) are shown in Table 1. The photopolymerized polymer was named PolyOSEA.

2.3 | Structural and Physico-Chemical Characterization

2.3.1 | Structure Determination

Fourier transform infrared (FTIR) spectroscopy was carried out using a Perkin-Elmer Spectrum 100 spectrometer equipped with an attenuated total reflectance (ATR) diamond accessory coated with a zinc selenide crystal. Spectra were recorded in the range of 600–4000 cm^{-1} with a resolution of 4 cm^{-1}, and 16 scans. ^{1}H NMR measurements were carried out using a Bruker AVANCE III spectrometer operating at 14.1 T and equipped with a 5 mm TCI cryoprobe and BBI probe head. All measurements were performed at 25°C, with samples dissolved in dimethylsulfoxide (DMSO).

2.3.2 | Rheological Analysis

The rheological tests on the SO, ESO, and OSEA samples were carried out on an Anton Paar MCR92 Rheometer. A 25 mm parallel plate geometry was used in the analyses to evaluate the viscosity of the samples as a function of time. The following parameters were used: 0.20 mm gap, 26°C temperature, and 0.01 rad/s for 240 s. A low shear rate was used in this analysis to avoid the influence of shear on the material's viscosity response.

2.3.3 | Water Absorption Rate

The samples were cut in 2 × 1 × 0.1 cm, weighed, and immersed in 5 mL of distilled water (pH = 6.8) at 25°C. The samples were withdrawn, their surface was gently dried with a soft paper, and weighed at 0.033, 0.083, 0.17, 0.25, 0.5, 1, 24, and 48 h. The water absorption rate was measured using the following equation: % water absorption rate $= (M_f \times 100)/M_i$, for which M_f is the final mass, and M_i is the initial mass. Triplicates of samples were tested for statistics, namely average and standard deviation (SD).

2.3.4 | Hydrolytic Degradation

The test was performed in triplicate using phosphate-buffered saline (PBS, pH 7.4 ± 0.2) for 6 weeks. The sample (2 × 1 × 0.1 cm) was weighed, inserted into test tubes with 5 mL of PBS, and maintained at room temperature. The samples were withdrawn, their surface was gently dried with a soft paper, and weighed at 0, 15, 30, and 45 days. The mass loss (%) was determined using the following equation: $\Delta M\% = ([M_0 - M_f] \times 100)/M_0$, for which ΔM is the weight loss, M_0 is the mass of the samples before the degradation test, and M_f is the mass of the samples at the different times. The hydrolytic degradation test was carried out in accordance with ASTM F1635-11 [23]. Triplicates of samples were tested for statistics, namely average and SD.

2.3.5 | Tensile Tests

Tensile tests were performed using a DL2000 universal testing machine (EMIC Instron) equipped with a 500 N load cell. Six samples (approximately 15 mm width × 1 mm thickness) were

TABLE 1 | AESO, *N, N*-dimethylacrylamide, and diphenylphosphoryl (mesityl)methanone amounts for optimization of the bioadhesive photopolymerization.

	AESO (g)	*N,N*-dimethylacrylamide (g)	Diphenylphosphoryl (mesityl)methanone (g)
Sample 1	0.3	0.3	0.06
Sample 2	0.3	0.6	0.09
Sample 3	0.6	0.3	0.09
Sample 4	0.6	0.3	0.045
Sample 5	0.9	—	0.045
Sample 6	0.9	—	0.09

tested at 6 mm.min^{-1}. All samples were conditioned at a relative humidity of 50% for 48 h at 23°C before testing. Young's modulus was determined as the slope at low deformation, and tensile strength was determined as the force of the sample at break. Six samples were tested for statistics, namely average and SD of deformation, Young's modulus and tensile stress.

2.3.6 | Cell Cytotoxicity Tests

The material's in vitro cytotoxicity was assessed using the resazurin-based assay, in which resorufin, the fluorescent product of resazurin reduction by cells, indicates cell viability. For this, L929 murine fibroblast cell culture was maintained at 37°C ± 2°C in a humidified atmosphere containing 5% CO_2 until they reached 80%–90% confluence, after which they were trypsinized. The resulting cell suspension was centrifuged for 5 min at 1200 × g, and 0.1 mL (1×10^5 cells) was seeded into each well of a 96-well microplate and incubated for 24 h. The culture medium was replaced with medium containing the sample extract (prepared by immersing the oil-based polymer in 1 mL of distilled water and incubating at 37°C for 24 h). The culture medium was used as a negative control (100% cell growth), and 10% (v/v) dimethylsulphoxide (DMSO) was used as a positive control. After 24 h of incubation with the test solutions extracted from the samples, the medium was removed and the cells were washed with PBS. Resazurin solution (10% vol) in DMEM supplemented with bovine serum was added to each well, and the plates were incubated for 4 h at 37°C ± 2°C in a 5% CO_2 atmosphere. The samples (100 μL) were transferred to the 96-well microplate, and the fluorescence was measured at an excitation wavelength of 570 nm and emission at 590 nm in a Cary Eclipse microplate reader (Agilent Technologies, Santa Clara, CA, USA). The test was carried out in triplicate. Cell viability was expressed as the relative percentage to the negative control. Data were processed using Microsoft Excel, and the results are shown as mean ± SD.

2.4 | Qualitative Wound Skin Adhesion Test

To simulate wound closure, we employed the methodology adapted from Fang et al. [5]. The skin used in the assays was of porcine origin, obtained from a local butcher. The material was stored under refrigeration at 2°C–8°C until use, ensuring its integrity. Samples measured 5 × 3 × 0.1 cm. On each sample, a linear incision 1 cm in length and approximately 1 mm in depth was made using a scalpel. The incision size was kept constant across all repetitions to ensure reproducibility of the assays. The adhesive polymer was applied in a controlled amount (100 μL), forming a thin layer on the outer surface of the skin. The material was then irradiated with UV light (Delpho Instruments, 400 nm, São Carlos, SP) for 70 s at a distance of 2 cm from the skin. The adhesion tests were carried out in two situations: (i) after application, with no time interval, and (ii) after complete polymer curing, the samples were submerged in a beaker containing water for 5 min. Following this period, the skin was carefully removed, gently dried with soft paper, and manually inspected to assess the adhesion of the bioadhesive.

3 | Results and Discussion

3.1 | Formulation, Handling Properties, and Curing Time of the Bioadhesive

In order to elucidate the appropriate proportions of the reagents for polymerization, their concentration was tested and the results are shown in Table 2. The curing time to generate the film was also carried out and the results ranged from 69 to 80 s. This curing time is interesting, as film formation in the wound area is critical for minimizing blood loss. Studies on citric acid-derived collagen sealants show adequate bonding strength and low toxicity; however, curing times of approximately 10 min, which is suboptimal for surgical applications. PolyOSEA curing time thus aligns well with these standards, further supporting its potential applicability in clinical medicine.

The literature describes the typical properties for bioadhesive, such as good flexibility, once it must adapt to the skin microstructure and be quick and easily handled, features found in surgical adhesives already used in medical practice [24], besides adequate adhesion. Following comparative analysis, Sample 3 was identified as the most promising formulation, displaying an optimal balance of malleability, adhesiveness, and rigidity. Consequently, it was selected as the reference formulation for following investigations, as illustrated in Figure 1.

3.2 | FTIR and ^{1}H RMN Results

FTIR spectroscopic results of SO, ESO, AESO, and the polymer are shown in Figure 2. The spectrum of soybean oil shows the typical strong absorption band at about 2800 and 2900 cm^{-1} corresponding to the stretching vibration of CH_2 and CH_3, and a strong band at about 1722 cm^{-1} attributed to its carbonyl (C═O) group. The ESO spectrum shows the new band at 818 cm^{-1} attributed to the epoxy group [25]. The disappearance of the band at 3008 cm^{-1}, corresponding to $H_2C{=}CH_2$ group, is also attributed to the epoxidation, confirming the success of the reaction. AESO spectrum displays bands at 980 and 1047 cm^{-1}, corresponding to CH vibrations, typical of acrylates, evidencing its insertion into the structure, even at a low degree. The spectrum of the polymer shows the carbonyl band at 1616 cm^{-1} and the appearance of the hydroxyl groups at about 3300 cm^{-1} indicating the crosslinking of the acrylate groups in the polymer, confirming the curing reaction [26, 27].

TABLE 2 | Curing time and malleability properties of bioadhesive.

Sample	Curing time (s)	Malleability
1	80	Low
2	71	Low
3	69	High
4	73	High
5	74	Low
6	72	Low

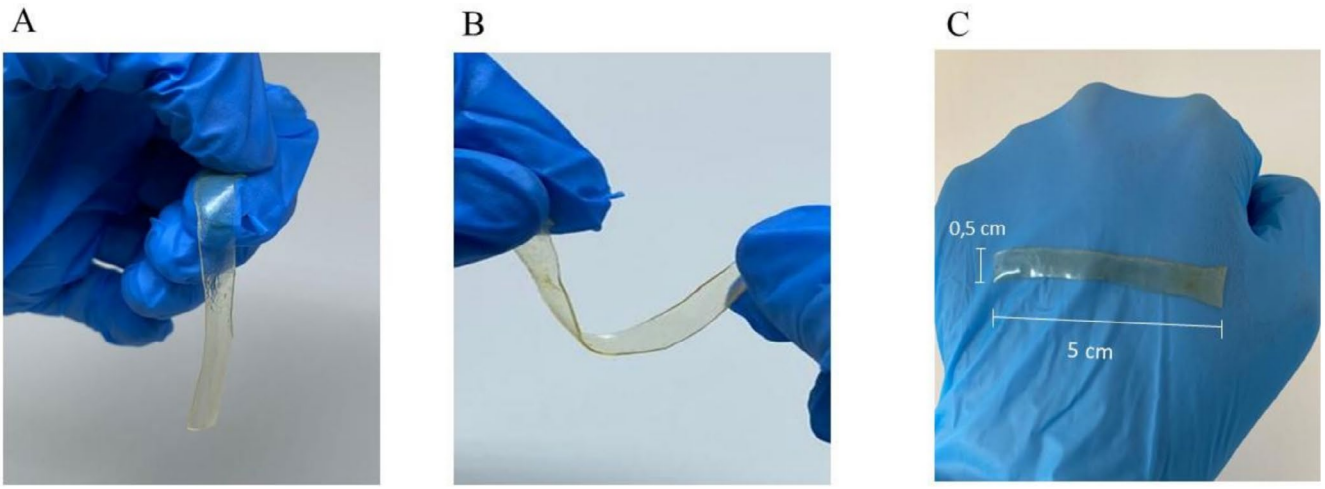

FIGURE 1 | Film made from sample 3 shown in images (A), demonstration of malleability (B), demonstration of adhesion of the material to a surface (C).

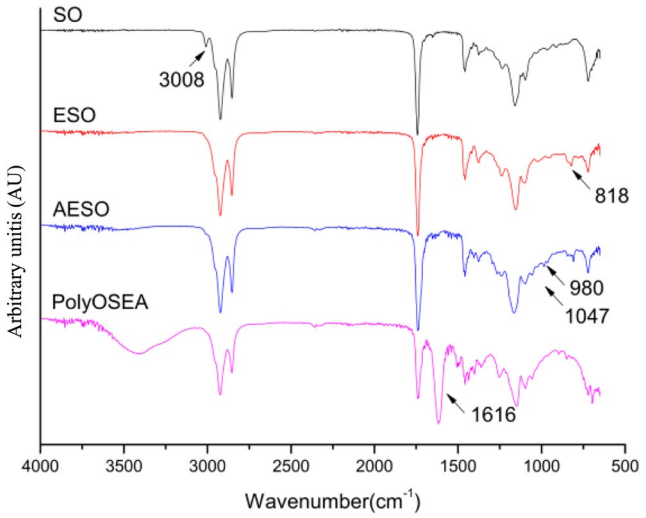

FIGURE 2 | FTIR spectra of soybean oil (SO), epoxidized soybean oil (ESO), acrylated epoxidized soybean oil (AESO), and the photopolymerized polymer (PolyOSEA).

The ^{1}H NMR spectra of the SO, ESO, and AESO are shown in Figure 3. The spectrum of soybean oil exhibits the typical peaks corresponding to the triglycerides structure. ESO peaks associated with epoxy protons appear at 2.91 ppm (j), and the protons adjacent to the epoxy group at 1.49 ppm (i). AESO peaks corresponding to acrylate protons, notably around 5.98–6.04 ppm (a), emerge. These spectral changes further confirm the successful epoxidation and subsequent acrylation of the soybean oil.

3.3 | Rheological Analysis

The rheological behavior of the samples is shown in Figure 4A and indicates the impact of chemical modification—epoxidation and acrylation—on the viscosity of soybean oil. The macroscopic differences between SO, ESO, and AESO are shown in Figure 4B. The viscosity of SO, ESO, and AESO slightly and gradually increased, respectively. The increased viscosity of ESO when compared to SO can be attributed to the epoxy groups in its structure, which increases its polarity and the intermolecular interactions between the chains. AESO displayed the highest viscosity. This higher viscosity can be attributed to the acrylated triglyceride molecules with a high content of polar hydroxyl groups and ester bonds associated with each acrylate moiety. These structural changes increase the intermolecular interactions among adjacent molecules, thus increasing the viscosity and showing that the chemical modifications influence the fluid dynamics of the soybean oil and its derivatives.

The modifications resulting from the epoxidation and acrylation processes also led the samples' color to change, as shown in Figure 5B. ESO appears more transparent than unmodified soybean oil, whereas AESO acquires a golden-yellow color as a possible result of the occurrence of the acrylation reaction.

3.4 | Water Absorption Rate, Hydrolytic Degradation, Cytotoxicity Test, and Mechanical Properties

The water absorption behavior of PolyOSEA, hydrolytic degradation, cytotoxicity, and the results of mechanical tests are shown in Figure 5. The results of the gravimetric analysis, presented in Figure 5A, showed that after 2 min of immersion, the PolyOSEA films had an initial water absorption of around 10.50%. During the first hour, this absorption increased to 33.33%. After 24 and 48 h, no significant variations were observed, with absorption values reaching 35.68% and 35.88%, respectively. This behavior indicates favorable performance, as the material maintains moisture while retaining structural integrity for at least 48 h. After this period of time, the film started to become brittle, possibly indicating the onset of hydrolytic degradation.

The results of hydrolytic degradation, Figure 5B, indicated a mass loss of about 16.92% after 15-day time point, followed by the loss of mass of about 24.65% at 30 days, and 28.88% at 45 days. These results can be attributed to the hydrolytic

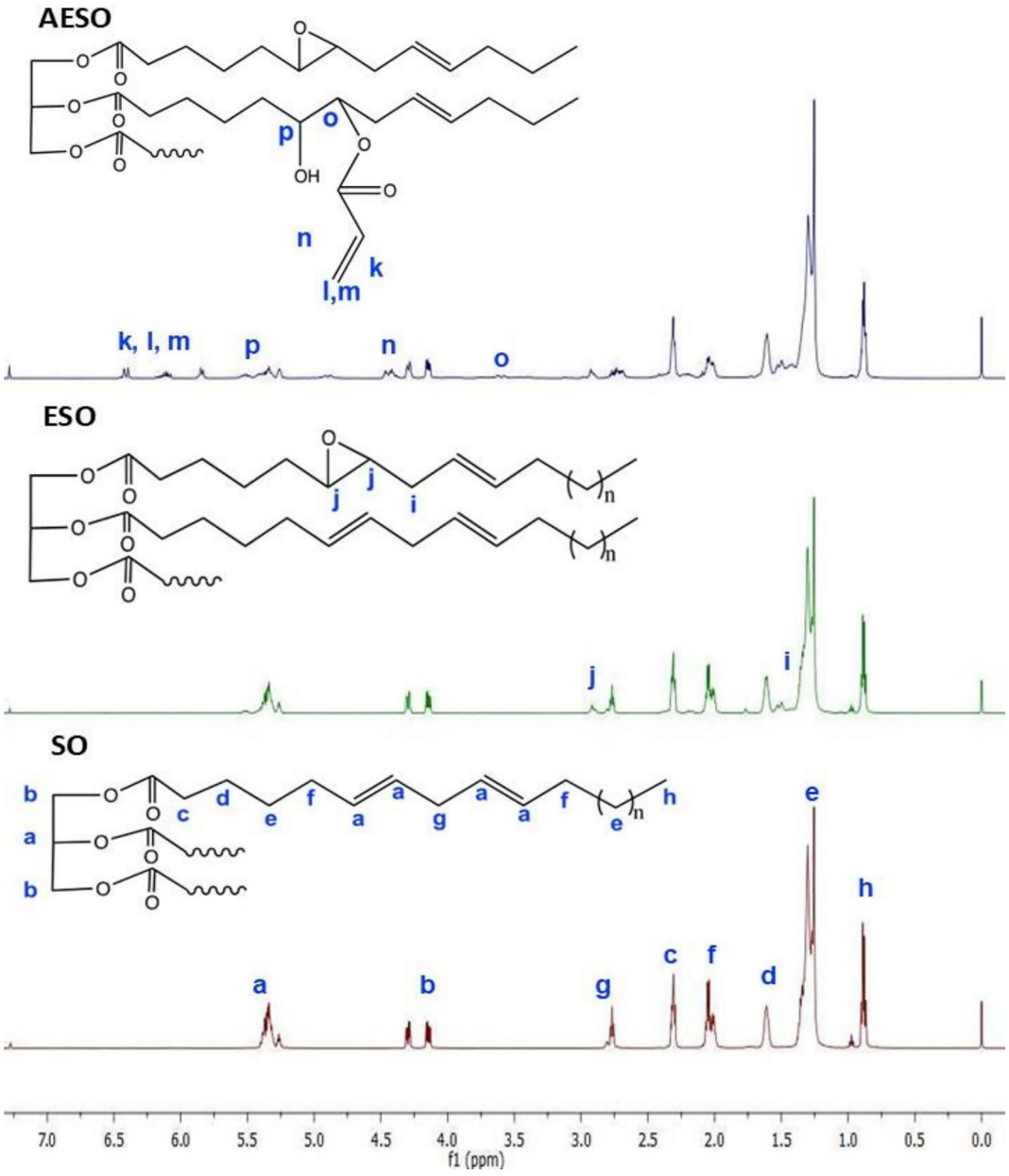

FIGURE 3 | ^{1}H RMN spectra of SO, ESO e AESO.

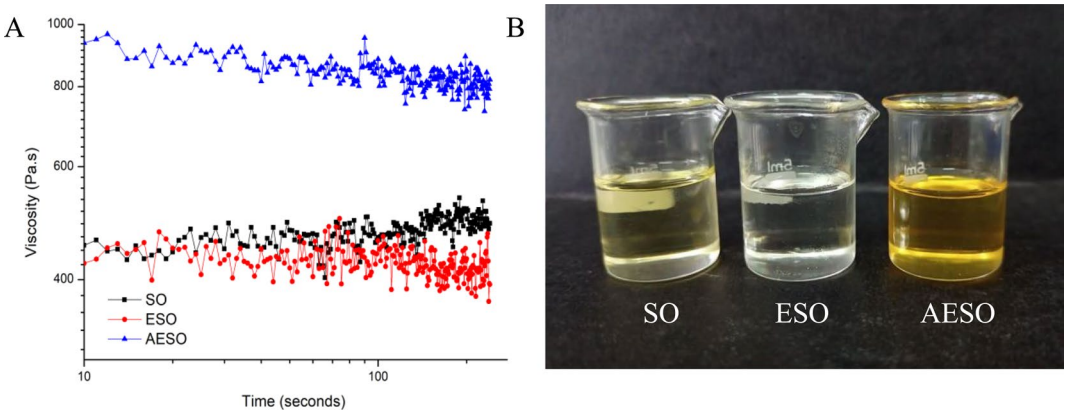

FIGURE 4 | Viscosity as a function of time for SO, ESO, and AESO, (A) differences between SO, ESO, and AESO (B).

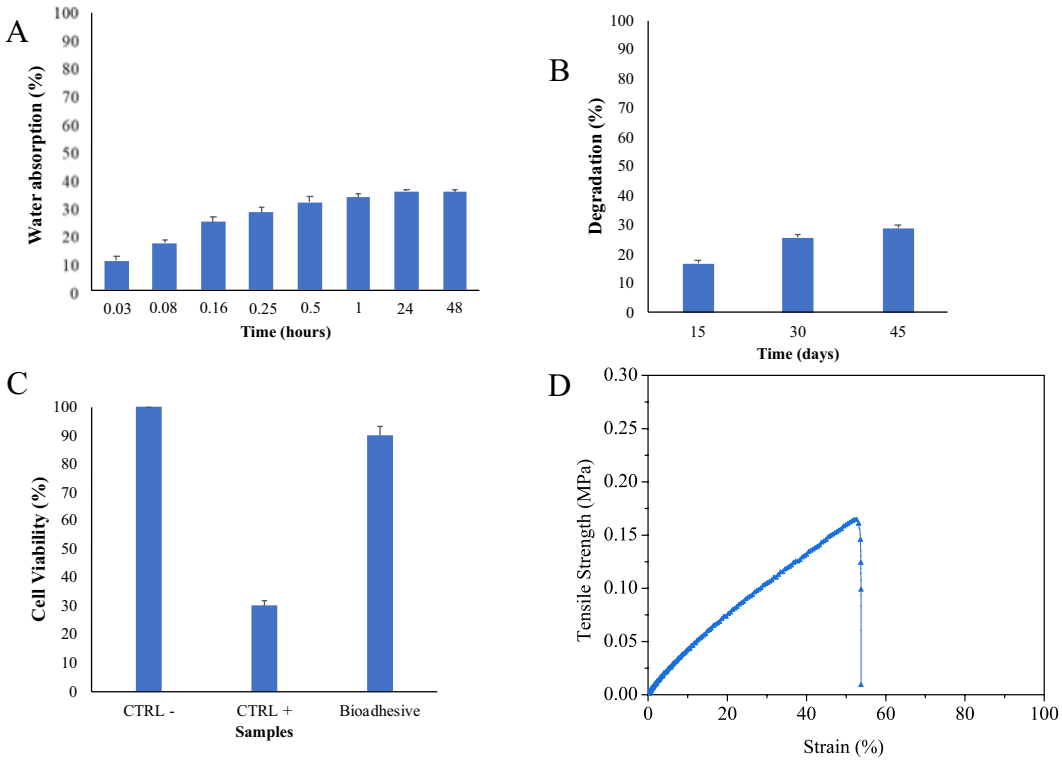

FIGURE 5 | Water absorption rate (A), degradation (B), and cell viability (C), and tensile tes results (D).

cleavage of the ester bonds in the polymer matrix and the leaching of the small broken molecules into the liquid. The immersion into phosphate-buffered saline led the matrix to swell, as shown in water absorption tests, thereby enhancing the hydrolytic degradation. Biodegradability is an important property for bioadhesives, mainly for those intended for internal use, as it influences both safety and functionality. Degradation may occur in vivo via enzymatic activity or more slowly via hydrolysis, as shown here. High hydrophilicity can accelerate the degradation, and high cross-linking density typically reduces the mass loss. Additionally, external influences, such as the specific conditions within the wound microenvironment, must be considered [28].

The cytotoxicity assay is used for determining if new materials intended for biomedical use can cause cell damage. According to the ISO 10993-5 standard, the cell viability above 70% is considered noncytotoxic [29]. The results indicated that the fibroblasts maintained normal viability of about 91.08% after 24 h of exposure to the PolyOSEA film and its extraction products. These results are shown in Figure 5C, which compares the viability of cells exposed to PolyOSEA with that of a control group.

Figure 5D shows the results of the mechanical tests. The Young's modulus, the tensile strength, and the elongation at break were determined from the stress–strain curves (Figure 5D). The result of tension assays shown for PolyOSEA is a nonlinear stress–strain curve, typical of elastomer materials, in which the tension increases slowly, reaching high elongation values (around 80%), followed by a gradual increase until break. The average Young's modulus was 0.348 ± 0.089 MPa, the average tensile strength was 0.165 ± 0.084 MPa, and the strain was 48.870% ± 16.315%.

3.5 | Qualitative Wound Skin Adhesion

Porcine skin was used to more show the bioadhesive's adhesion capability, and the results are shown in Figure 6. This model was chosen because of the similarity between porcine skin and human skin, both in terms of structure and composition. Anatomically and physiologically, porcine skin has similar features to human skin, such as the thick epidermis and the comparable dermis–epidermis ratio [15], leading to more reliable results. The bioadhesive exhibited adhesion to the skin surface and was capable of approximating the cut tissues, putting them in contact (Figure 6B). This result can indicate the potential of the material to improve the healing process. Furthermore, after contact with water for 10 min, the bioadhesive remained stable and firmly adhered to the skin, without losing the tissue approximation capability. This result complements the potential of the material for application to joint incisions, where the resistance to moisture absorption is essential to guarantee its effectiveness and safety.

The adhesion force between PolyOSEA and the porcine skin was qualitatively tested by hand. The samples were not measured using the standard adhesion test because of the low fitting capability of the porcine skin into the tensile test grip machine, thus representing a limitation of this work.

4 | Discussion

Bioadhesives have transformed surgical practice over the last 30 years, with increasing clinical interest and an estimated market value of US$ 38 billion [30]. Their applications include surgical wound closure, fixation of implantable devices, and the promotion of hemostasis [31].

Curing time is a critical parameter and may rely on chemical cross-linking, heat, mechanical fixation, or photopolymerization, depending on the formulation and intended use. Photopolymerization has emerged as a promising approach due to its rapidity, low cost, solvent-free nature, and mild reaction conditions. Nevertheless, curing time must be carefully controlled to ensure effective adhesion and mechanical stability: excessively short curing times may compromise adhesive strength, whereas longer curing periods can prolong surgical procedures and increase infection risk due to extended wound exposure. Indeed, the literature demonstrates that adequate curing times are essential for achieving optimal adhesion and mechanical performance in clinical applications [32, 33]. For epoxidized soybean oil-based bioadhesives, curing times range from approximately 40 s under near-infrared laser irradiation (808 nm, 0.2 W cm^{-2}) [34] to 30 s with UV LED exposure (380–390 nm, 40 W) [13]. By comparison, cyanoacrylate adhesives typically polymerize in around 60 s, driven by an exothermic reaction [6]. In this study, the observed curing time of ~80 s can therefore be considered clinically acceptable when compared with these reported benchmarks.

Another determinant of bioadhesive performance is the ability to form an adequate interfacial bond with the target tissue [30]. The adhesive must remain securely attached to the tissue surface while avoiding damage during manipulation or removal. Adhesion arises from the interplay between adhesive and cohesive forces, with tissue–adhesive interactions being mediated by functional groups naturally present on the skin, such as amino, hydroxyl, carboxyl, and sulphydryl groups [35, 36]. These groups provide potential binding sites, as illustrated schematically in Figure 7.

The degradation profile of clinically available bioadhesives is strongly influenced by their chemical composition and molecular structure. Parameters such as polymer hydrophilicity, cross-link density, and local pH modulate degradation kinetics [37]. Cyanoacrylates represent the earliest synthetic materials used for wound closure, with Dermabond being one of the most recognized commercial products. Since 1998, octyl-2-cyanoacrylate has been FDA-approved and widely adopted owing to its rapid polymerization and strong skin adhesion. Importantly, the degradation rate of cyanoacrylate-based adhesives depends on the alkyl chain length: shorter chains, such as ethyl cyanoacrylate, degrade more rapidly, while longer chains, such as octyl cyanoacrylate, provide slower degradation [38]. For clinical viability, the degradation rate must align with tissue repair dynamics, maintaining structural support without hindering healing or predisposing to infection. The slow degradation behavior observed for PolyOSEA

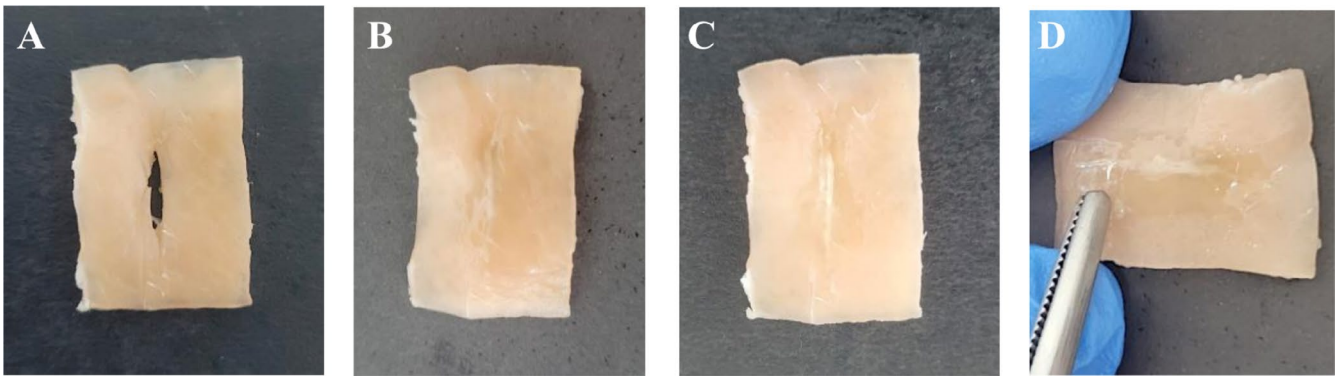

FIGURE 6 | Porcine skin incision (A), porcine skin with light-cured soybean oil over the incision (B), porcine skin with light-cured soybean oil over the incision after immersion in water (C) and manual analysis of adhesion after immersion in water (D).

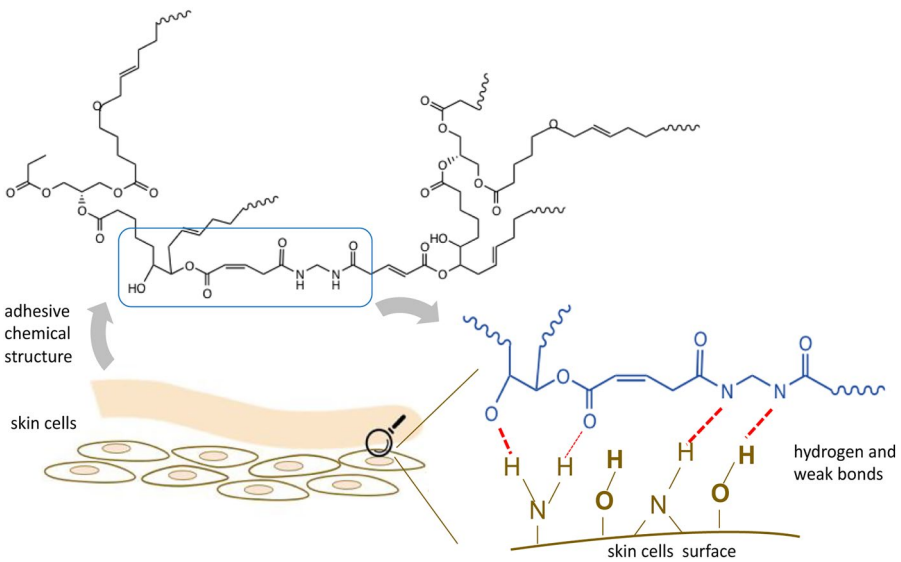

FIGURE 7 | Bioadhesive adhesion to tissue mechanism.

suggests suitability for medical use, as it preserves adhesive function without compromising healing [39].

Despite these promising results, certain limitations remain common to surgical bioadhesives. These include reduced efficacy in wet surgical fields, potential biocompatibility concerns, and the scalability of photopolymerization processes. In particular, achieving uniform curing in larger adhesive volumes is a manufacturing challenge that could compromise product consistency. Another critical consideration is compatibility with sterilization procedures, as clinical use requires effective sterilization without altering material properties. Methods such as autoclaving or ethylene oxide exposure have been shown to reduce stiffness in methacryloyl gelatin (GelMA)-based hydrogels, whereas gamma irradiation may increase stiffness and delay biodegradation [40]. Heinemann et al. further demonstrated that gamma irradiation of photopolymerized hyaluronic acid and GelMA hydrogels reduced the elastic modulus and altered dissolution behavior [41]. These findings highlight the need for systematic evaluation of sterilization protocols for PolyOSEA to ensure stability, safety, and reproducibility in clinical settings.

5 | Conclusions

The study shows the development of a photo-curable soybean oil-based polymer (PolyOSEA) with potential application as a bioadhesive, as a potential alternative to sutures and conventional wound protectants. Among the formulations tested, PolyOSEA exhibited good features, including a curing time of approximately 69 s. Water absorption analysis revealed moderate uptake within the first 24 h, followed by stabilization after 48 h, supporting the maintenance of a moist wound environment. Cytotoxicity testing confirmed the material's biocompatibility, with a high cell viability rate of 91.08%. These results indicate that PolyOSEA has great potential for application as a surgical adhesive or even a wound dressing, contributing to the advancement of biomedical materials and tissue engineering. Future studies should include in vivo evaluation of biocompatibility, degradation kinetics, and the effectiveness of the bioadhesive in the wound healing process, as well as histopathological analysis of tissue response and possible inflammation. However, this is a proof-of-concept study, and further testing is needed to validate its efficacy and safety before possible clinical translation.

Acknowledgments

The authors thank Fapesp for the grant 2017-18782-6 and 2019/25316-7, CNPq grant number 305518/2023-2, and CAPES for Tatiane Araujo Soares PhD grant 88870713632/2022-00. The Article Processing Charge for the publication of this research was funded by the Coordenação de Aperfeiçoamento de Pessoal de Nível Superior - Brasil (CAPES) (ROR identifier: 00x0ma614).

Ethics Statement

The authors have nothing to report.

Conflicts of Interest

The authors declare no conflicts of interest.

Data Availability Statement

The data that support the findings of this study are available from the corresponding author upon reasonable request.

References

1. A. Bal-Ozturk, B. Cecen, M. Avci-Adali, et al., "Tissue Adhesives: From Research to Clinical Translation," *Nano Today* 36 (2021): 101049, https://doi.org/10.1016/j.nantod.2020.101049.

2. C. V. S. González, E. O. D. Carvalho, N. S. Galvão, P. C. Nogueira, and V. L. C. D. G. Santos, "Prevalence of Complicated Surgical Wounds and Related Factors Among Adults Hospitalized in Public Hospitals," *Revista da Escola de Enfermagem da USP* 56 (2022): e20210477, https://doi.org/10.1590/1980-220X-REEUSP-2021-0477en.

3. S. V. Patel, D. D. Paskar, R. L. Nelson, S. S. Vedula, and S. R. Steele, "Closure Methods for Laparotomy Incisions for Preventing Incisional Hernias and Other Wound Complications," *Cochrane Database of Systematic Reviews* 11, no. 11 (2017): CD005661, https://doi.org/10.1002/14651858.CD005661.pub2.

4. Q. Su, D. Wei, W. Dai, Y. Zhang, and Z. Xia, "Designing a Castor Oil-Based Polyurethane as Bioadhesive," *Colloids and Surfaces B: Biointerfaces* 181 (2019): 740–748, https://doi.org/10.1016/j.colsurfb.2019.06.032.

5. Y. Fang, Y. Zheng, C. Chi, et al., "PAA-PU Janus Hydrogels Stabilized by Janus Particles and Its Interfacial Performance During Hemostatic Processing," *Advanced Healthcare Materials* 13, no. 13 (2024): 2303802, https://doi.org/10.1002/adhm.202303802.

6. Z. Bao, M. Gao, Y. Sun, R. Nian, and M. Xian, "The Recent Progress of Tissue Adhesives in Design Strategies, Adhesive Mechanism and Applications," *Materials Science and Engineering* 111 (2020): 110796, https://doi.org/10.1016/j.msec.2020.110796.

7. G. G. Hallock, "Expanded Applications for Octyl-2-Cyanoacrylate as a Tissue Adhesive," *Annals of Plastic Surgery* 46 (2001): 185–189.

8. M. Uccelli, S. Targa, G. C. Cesana, et al., "Use of Fibrin Glue in Bariatric Surgery: Analysis of Complications After Laparoscopic Sleeve Gastrectomy on 450 Consecutive Patients," *Updates in Surgery* 73 (2021): 305–311, https://doi.org/10.1007/s13304-020-00865-9.

9. N. Annabi, K. Yue, A. Tamayol, and A. Khademhosseini, "Elastic Sealants for Surgical Applications," *European Journal of Pharmaceutics and Biopharmaceutics* 95 (2015): 27–39, https://doi.org/10.1016/j.ejpb.2015.05.022.

10. I. Cryolife, "BioGlue Surgical Adhesive. In: Cryolife, Inc. Biotechnologies for Medicine," 2005, http://www.cryolife.com.br.

11. K. Despoudi, I. Mantzoros, O. Ioannidis, et al., "The Effect of Albumin/Glutaraldehyde Glue (Bioglue) on Colonic Anastomosis Under Intestinal Obstruction: An Experimental Study in Rats," *Journal of Clinical Medicine* 14, no. 7 (2025): 2457, https://doi.org/10.3390/jcm14072457.

12. R. D. O'Rorke, O. Pokholenko, F. Gao, et al., "Addressing Unmet Clinical Needs With UV Bioadhesives," *Biomacromolecules* 18, no. 3 (2017): 674–682, https://doi.org/10.1021/acs.biomac.6b01743.

13. Z. Wang, T. Wu, S. Yu, et al., "Biodegradable Plant Oil-Based Bioadhesive With Ultrastrong Wet-Tissue Adhesion for Instant Sealing Hemostasis," *ACS Applied Materials & Interfaces* 16, no. 31 (2024): 40653–40666, https://doi.org/10.1021/acsami.4c07517.

14. I. Eshkol-Yogev, T. Tobias, A. Keren, et al., "Dual Composite Bioadhesives for Wound Closure Applications: An In Vitro and In Vivo Study," *Polymers for Advanced Technologies* 33, no. 11 (2022): 3862–3877, https://doi.org/10.1002/pat.5691.

15. A. Neiman, I. Eshkol-Yogev, A. Keren, et al., "Closure of Long Surgical Incisions With Hemostatic Tissue Adhesive in a Porcine Skin Model," *Advances in Skin & Wound Care* 36, no. 10 (2023): 1–10, https://doi.org/10.1097/ASW.0000000000000036.

16. M. A. Meier, J. O. Metzger, and U. S. Schubert, "Plant Oil Renewable Resources as Green Alternatives in Polymer Science," *Chemical Society Reviews* 36 (2007): 1788–1802, https://doi.org/10.1039/b703294c.

17. H. Esen and G. Çayli, "Epoxidation and Polymerization of Acrylated Castor Oil," *European Journal of Lipid Science and Technology* 118 (2016): 959–966, https://doi.org/10.1002/ejlt.201500132.

18. O. Awogbemi, E. I. Onuh, and F. L. Inambao, "Comparative Study of Properties and Fatty Acid Composition of Some Neat Vegetable Oils and Waste Cooking Oils," *International Journal of Low-Carbon Technologies* 14 (2019): 417–425, https://doi.org/10.1093/ijlct/ctz038.

19. G. V. Olivieri, J. J. V. Quadros, and R. Reinaldo Giudici, "Epoxidation Reaction of Soybean Oil: Experimental Study and Comprehensive Kinetic Modeling," *Industrial & Engineering Chemistry Research* 59 (2021): 18808–18823, https://doi.org/10.1021/acs.iecr.0c03847.

20. R. Saraswat, Shagun, A. Dhir, A. S. S. Balan, S. Powar, and M. Doddamani, "Synthesis and Application of Sustainable Vegetable Oil-Based Polymers in 3D Printing," *RSC Sustainability* 2 (2024): 1708–1737, https://doi.org/10.1039/d4su00060a.

21. M. Kaur and A. K. Srivastava, "Photopolymerization: A Review," *Journal of Macromolecular Science, Part C: Polymer Reviews* 42 (2002): 481–512, https://doi.org/10.1081/MC-120015988.

22. A. B. Kousaalya, B. Ayalew, and S. Pilla, "Photopolymerization of Acrylated Epoxidized Soybean Oil: A Photocalorimetry-Based Kinetic Study," *ACS Omega* 4, no. 26 (2019): 21799–21808, https://doi.org/10.1021/acsomega.9b02680.

23. American Society for Testing and Materials—ASTM, *ASTM F1635-11: Standard Test Method for In Vitro Degradation Testing of Hydrolytically Degradable Polymer Resins and Fabricated Forms for Surgical Implants* (ASTM, 2010).

24. Q. Wu, Y. Hu, J. Tang, et al., "High-Performance Soybean-Oil-Based Epoxy Acrylate Resins:"Green" Synthesis and Application in UV-Curable Coatings," *ACS Sustainable Chemistry & Engineering* 6 (2018): 8340–8349, https://doi.org/10.1021/acssuschemeng.8b00388.

25. J. Dai, X. Liu, S. Ma, et al., "Soybean Oil-Based UV-Curable Coatings Strengthened by Crosslink Agent Derived From Itaconic Acid Together With 2-Hydroxyethyl Methacrylate Phosphate," *Progress in Organic Coatings* 97 (2016): 210–215, https://doi.org/10.1016/j.porgcoat.2016.04.014.

26. F. Habib and M. Bajpai, "Synthesis and Characterization of Acrylated Epoxidized Soybean Oil for UV Cured Coatings," *Chemistry & Chemical Technology* 5 (2011): 317–326, https://doi.org/10.23939/chcht05.03.317.

27. A. N. Mendes, J. R. Gregório, and R. G. D. Rosa, "Studies on the Experimental Variables Effects on Rhodium Catalyzed Hydroformylation of Unsaturated Fatty Esters and Comparison of [RhH (CO)(PPh3) 3] and [RhCl3. 3H2O] as Starting Catalytic Precursors," *Journal of the Brazilian Chemical Society* 16 (2005): 1124–1129, https://doi.org/10.1590/S0103-50532005000700006.

28. D. Hansen, J. Eiler, K. Hansen, and E. Thormann, "Dynamics of Water Absorption in Polymer Skin Adhesives," *ACS Applied Bio Materials* 3 (2020): 8698–8704, https://doi.org/10.1021/acsabm.0c01089.

29. "ISO 10993-5:2009: Biological Evaluation of Medical Devices—Part 5: Tests for In Vitro Cytotoxicity."

30. W. Duan, X. Bian, and Y. Bu, "Applications of Bioadhesives: A Mini Review," *Frontiers in Bioengineering and Biotechnology* 9 (2021): 716035, https://doi.org/10.3389/fbioe.2021.716035.

31. B. Xue, J. Gu, L. Li, et al., "Hydrogel Tapes for Fault-Tolerant Strong Wet Adhesion," *Nature Communications* 12, no. 1 (2021): 7156, https://doi.org/10.1038/s41467-021-27529-5.

32. S. Genty, P. Tingaut, and M. Aufray, "Fast Polymerization at Low Temperature of an Infrared Radiation Cured Epoxy-Amine Adhesive," *Thermochimica Acta* 666 (2018): 27–35, https://doi.org/10.1016/j.tca.2018.05.018.

33. K. Uma, "Bioadhesives for Clinical Applications–a Mini Review," *Materials Advances* 4, no. 9 (2023): 2062–2069, https://doi.org/10.1039/D2MA00941B.

34. Z. Wang, T. Wu, F. Zhao, et al., "An Injectable Epoxidized Soybean Oil/Gelatin-Based Photothermal Biogel With Remarkable Rapid Hemostasis Capability for Wound Repair," *International Journal of Biological Macromolecules* 283 (2024): 137902, https://doi.org/10.1016/j.ijbiomac.2024.137902.

35. Y. Ding, L. Yu, and Z. Mao, "Adhesion Mechanisms and Design Strategies for Bioadhesives," *Colloid and Interface Science Communications* 63 (2024): 100809, https://doi.org/10.1016/j.colcom.2024.100809.

36. M. H. Ho, Q. van Hilst, X. Cui, et al., "From Adhesion to Detachment: Strategies to Design Tissue-Adhesive Hydrogels," *Advanced NanoBiomed Research* 4 (2024): 2300090, https://doi.org/10.1002/anbr.202300090.

37. M. Nakipoglu, A. Tezcaner, C. H. Contag, N. Annabi, and N. Ashammakhi, "Bioadhesives With Antimicrobial Properties," *Advanced Materials* 35, no. 49 (2023): 2300840, https://doi.org/10.1002/adma.202300840.

38. L. Sanders and J. Nagatomi, "Clinical Applications of Surgical Adhesives and Sealants," *Critical Reviews in Biomedical Engineering* 42, no. 3–4 (2014): 271–292, https://doi.org/10.1615/critrevbiomedeng.2014011676.

39. S. Zhu, W. Dou, X. Zeng, et al., "Recent Advances in the Degradability and Applications of Tissue Adhesives Based on Biodegradable Polymers," *International Journal of Molecular Sciences* 25 (2024): 5249, https://doi.org/10.3390/ijms25105249.

40. F. Zhang, G. Scull, J. M. Gluck, A. C. Brown, and M. W. King, "Effects of Sterilization Methods on Gelatin Methacryloyl Hydrogel Properties and Macrophage Gene Expression In Vitro," *Biomedical Materials* 18, no. 1 (2022): 015015, https://doi.org/10.1088/1748-605X/aca4b2.

41. C. Heinemann, F. Buchner, P. S. Lee, et al., "Effects of Gamma Irradiation and Supercritical Carbon Dioxide Sterilization on Methacrylated Gelatin/Hyaluronan Hydrogels," *Journal of Functional Biomaterials* 14, no. 6 (2023): 317, https://doi.org/10.3390/jfb14060317.